



Short communication

Dynamic electrochemical impedance spectroscopy reconstructed from continuous impedance measurement of single frequency during charging/discharging



Jun Huang, Zhe Li, Jianbo Zhang*

Department of Automotive Engineering, State Key Laboratory of Automotive Safety and Energy, Tsinghua University, Beijing 100084, PR China

HIGHLIGHTS

- Dynamic EIS was reconstructed from continuous impedance measurement of single frequency during charging/discharging.
- The charge transfer resistance from DEIS was generally smaller than that from SEIS.
- The charge transfer resistance during charging was generally smaller than that during discharging.

ARTICLE INFO

Article history:

Received 17 April 2014

Received in revised form

10 July 2014

Accepted 11 July 2014

Available online 18 July 2014

Keywords:

Lithium-ion battery

Dynamic electrochemical impedance spectroscopy

Single frequency impedance

Charge and discharge differences

ABSTRACT

In this study, a novel implementation of dynamic electrochemical impedance spectroscopy (DEIS) is proposed. The method first measures the impedance continuously at a single frequency during one charging/discharging cycle, then repeats the measurement at a number of other selected frequencies. The impedance spectrum at a specific SOC is obtained by interpolating and collecting the impedance at all of the selected frequencies. The charge transfer resistance, R_{ct} , from the DEIS is smaller than that from the steady EIS in a wide state-of-charge (SOC) range from 0.4 to 1.0, the R_{ct} during charging is generally smaller than that during discharging for the battery chemistry used in this study.

© 2014 Published by Elsevier B.V.

1. Introduction

Electrochemical impedance spectroscopy (EIS), capable of separating various processes of different time scales, provides valuable insights into electrochemical characteristics of the lithium-ion batteries. In most of the previous studies [1,2], the EIS was measured at stationary state (SEIS), i.e. the DC current is zero, to fulfill the requirements of the stability, linearization and causality. Then, the obtained EIS data were used to study the intercalation processes at the electrode/electrolyte interphase [3], or to simulate and predict the battery performance such as the state-of-charge (SOC) estimation in the battery management system (BMS) [4], etc. One drawback of the SEIS is that it cannot distinguish the differences between charging and discharging, since both the charging and discharging process occur in one cycle of the

alternating current. Itagaki et al. revealed that the solid electrolyte interphase (SEI) film resistance during charging is twice as that during discharging in the first few cycles [6,7]. Zhang et al. found that, the overpotential resistances to calculate the heat generation rate are different from charging to discharging [5].

In 1985, Stoynov et al. [8] conducted the impedance study of non-stationary systems for the first time. Afterward, in 1989, Chenebault et al. [9] measured the impedance of a Li metal electrode in $\text{LiAlCl}_4/\text{SOCl}_2$ electrolyte while the system was under charging. DEIS was later introduced to lithium metal battery by Osaka et al., in 1994 [10], and to lithium-ion battery by Itagaki et al., in 2004 [6,7]. It has also been applied to corrosion science [11] and fuel cell technology [12].

It is ideal to capture the impedance response of multiple frequencies during dynamic process at the same SOC. However, since the battery system is under nonstationary state, the SOC at the beginning and the ending of DEIS are different, thus, the DEIS is obtained across an SOC interval. Two methods have been proposed to consider or reduce the SOC change during the impedance

* Corresponding author.

E-mail address: jbzhang@mail.tsinghua.edu.cn (J. Zhang).

measurement. The first method assumes the battery's state and parameter's spaces are continuous and then introduces a time axis besides the real and imaginary one [6–8]. In this way, one can account for the SOC variation by interpolating at one time point to obtain the impedance spectrum at a specific SOC point. The second method is to reduce the measurement time and the SOC variation by measuring the impedance spectrum with simultaneous excitation of multiple perturbation frequencies, this method have been successfully implemented in Ref. [11].

In this study, we introduce a novel implementation of DEIS method for lithium-ion battery to eliminate the SOC change during DEIS test. This method conducts continuous impedance measurement of a single frequency on a full SOC range during charging or discharging, respectively. It then repeats the measurement at other selected frequencies. Finally, the impedance spectrum at all of the different frequencies could be combined and extracted at each specific SOC point during charging or discharging respectively. Using the proposed method, we explore the differences between SEIS and DEIS, and the differences between charging and discharging reactions.

2. Experimental

The DEIS measurement was conducted for a commercial 18,650 cell. The cell specifications are shown in Fig. 1(a). Before the DEIS tests, the cell was subjected to five conditioning cycles using constant current (CC) pattern, that is, the cell was charged to 4.2 V with a constant current (1 A), defined as SOC = 1.0; and then, after a rest period at open circuit of 1 h, the cell was discharged to 3.0 V with the same current, defined as SOC = 0. After this, the DEIS tests were performed with the parameters shown in Fig. 1(b). When measuring the DEIS, the cell was under constant current (1 A) charging/discharging, while simultaneously a sinusoidal current with a small magnitude (0.01 A) was superimposed. Note that the impedance of each single frequency was measured continuously from SOC = 0 to SOC = 1.0 during charging and from SOC = 1.0 to

SOC = 0 during discharging. Fig. 1(c) depicts the schematic of the current profile and the corresponding voltage response. Conventional SEIS tests were measured with a sinusoidal excitation of 0.01 A over the frequency range of 10^4 – 10^{-1} Hz from SOC = 0 to SOC = 1.0 with a step of 0.1 to compare the DEIS. All the conditioning cycles and EIS tests, including both steady and dynamic EIS, were conducted with an *Autolab PGSTAT302N* impedance analyzer (Eco Chemie, Netherland). An environment chamber GDJW-225 was used to provide constant temperature environment in all the tests.

3. Results and discussion

3.1. Continuous impedance of single frequency during cycling

Fig. 2 shows the continuous impedance of each frequency from SOC = 1.0 to SOC = 0 at 20 °C during charging (a) and discharging (b). Z' and Z represent the real and imaginary part of impedance, respectively.

Firstly, we analyze the real part of the impedance. (1) with respect to the relationship between impedance and the SOC, one can notice that: during the charging process, Z' increases monotonically with lowering the SOC; during the discharging process, however, Z' exhibits a non-monotonic behavior. Z' decreases at the beginning of discharge and then increases with decreasing the SOC. At the ending of discharge, Z' decreases at low frequencies (10 Hz–1 Hz); (2) with regard to the relationship between the impedance and the frequency, Z' increases monotonically with lowering the frequency both during charging and discharging. Besides, Z' rises steeply near SOC = 0 at low frequencies (10 Hz–1 Hz).

Secondly, we focus on the imaginary part of the impedance. (1) with respect to the relationship between the impedance and the SOC, one can find that: Z increases monotonically when lowering the SOC during the charging process, while, during the discharging process, Z shows a more complex nature which depends on the frequency. At high frequencies (1000 Hz–100 Hz), Z keeps

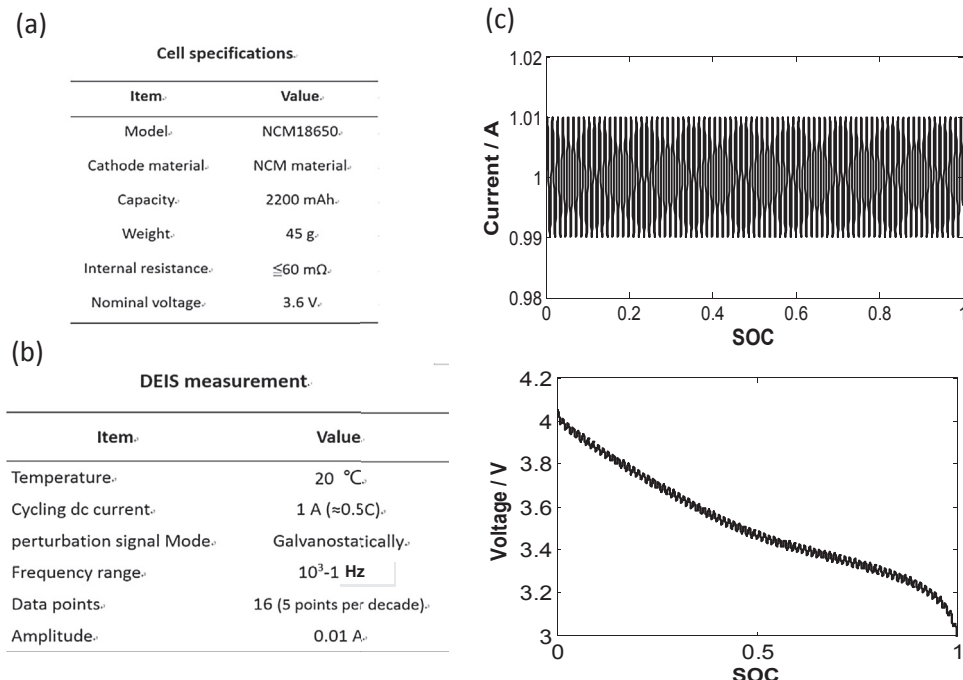


Fig. 1. (a) Specifications of the experimental cell, (b) the parameters of the DEIS measurement, (c) a representative current profile of a specific frequency and its corresponding voltage response (discharging for example).

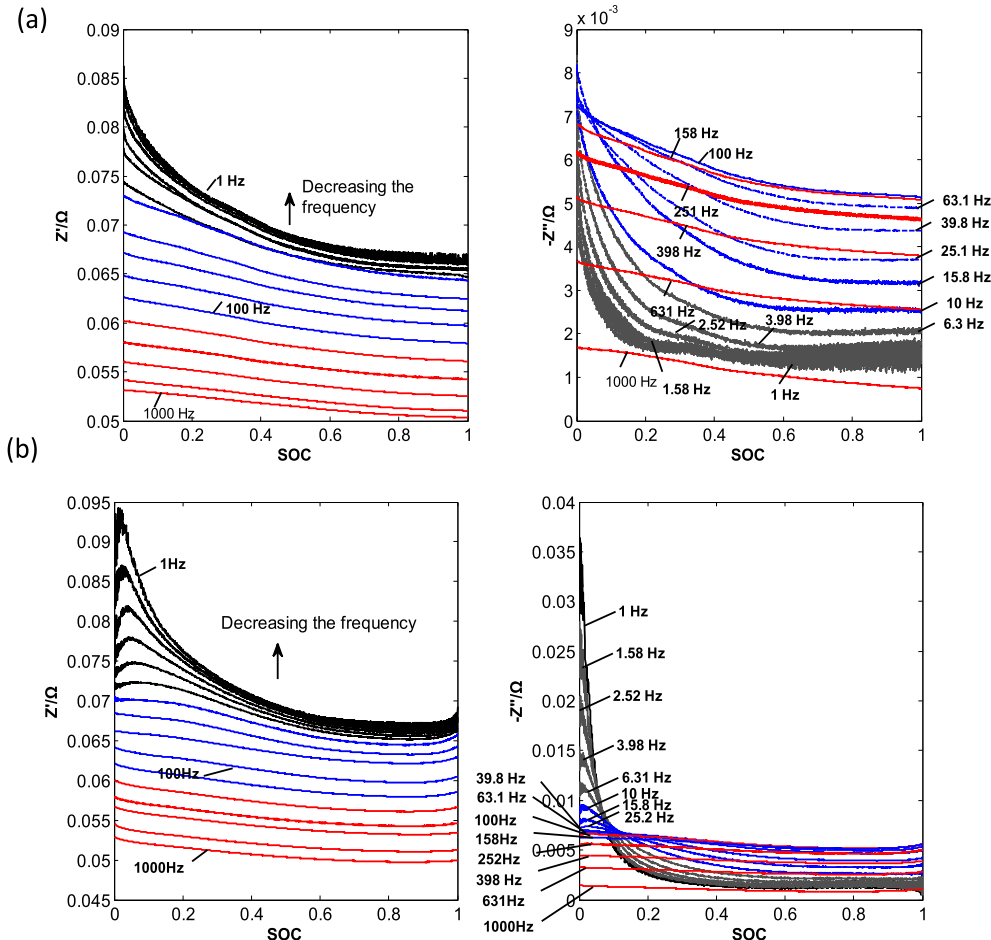


Fig. 2. The continuous impedance of each frequency during charging (a) and discharging (b). Z' and Z'' represent the real and imaginary part of impedance, respectively. The frequencies between 1000 Hz and 158 Hz, 100 Hz–15.8 Hz and 10 Hz–1 Hz are marked as red, blue, black lines, respectively. (For interpretation of the references to color in this figure legend, the reader is referred to the web version of this article.)

approximately constant with decreasing the SOC. At low frequencies (100 Hz–1 Hz), Z decreases at the beginning of discharging and then ascends slightly on the SOC range of 0.8 to 0.2, finally, Z rises steeply near the fully discharged state; (2) with regard to the relationship between impedance and the frequency, Z increases when lowering the frequency from 1000 Hz to 100 Hz both during discharging and charging, contrarily, decreases when further lowering the frequency from 100 Hz to 1 Hz. Exception only occurs near SOC = 0 where Z of lower frequencies may exceed that of 100 Hz.

3.2. Impedance spectrum at each specific SOC during charging and discharging

The impedance spectrum at different frequencies on the full SOC range were combined and then, we extracted the impedance spectrum at eleven SOC points from 1.0 to 0 in a step of 0.1 during charging and discharging, respectively, by interpolation. Fig. 3(a) shows the obtained DEIS both of charging and discharging, and compares them with the SEIS results.

It is clear that by conducting the continuous single frequency impedance measurement during cycling repeatedly, the impedance spectrum at each specific SOC point could be obtained both for charging and discharging process. This method has successfully overcome the problem of SOC variation during the DEIS measurement. Three main findings can be seen from Fig. 3:

- (1) *The DEIS is generally smaller than the SEIS.* Similar results have been reported previously by measuring the DEIS step by step with perturbation signals of different frequencies [13]. Ref. [13] points out that the difference between DEIS and SEIS could be largely attributed to the differences of the charge transfer resistance, R_{ct} . Using the equivalent electric circuit (EEC) in Fig. 3(b), we can fit the impedance spectrum and then extract the R_{ct} both for the DEIS and the SEIS at 11 SOC points. As shown in Fig. 3(c), the R_{ct} of DEIS is generally smaller than that of SEIS, except when the SOC is smaller than 0.4 during discharging process.

Based on the Butler–Volmer equation, R_{ct} correlates with the overpotential, η , as follows:

$$R_{ct} = \frac{1}{ai_0 \left[\frac{\alpha F}{RT} \exp\left(\frac{\alpha F}{RT} \eta\right) + \frac{(1-\alpha)F}{RT} \exp\left(-\frac{(1-\alpha)F\eta}{RT}\right) \right]} \quad (1)$$

where a is the active surface area, i_0 the exchange current density, depending on the concentration of lithium-ions at the surface of the active materials, η the overpotential, α the transfer coefficient, n the number of electrons per molecule reduced or oxidized, which equals 1 in this specific system, F Faraday's constant, R the gas constant, and T the absolute temperature in K.

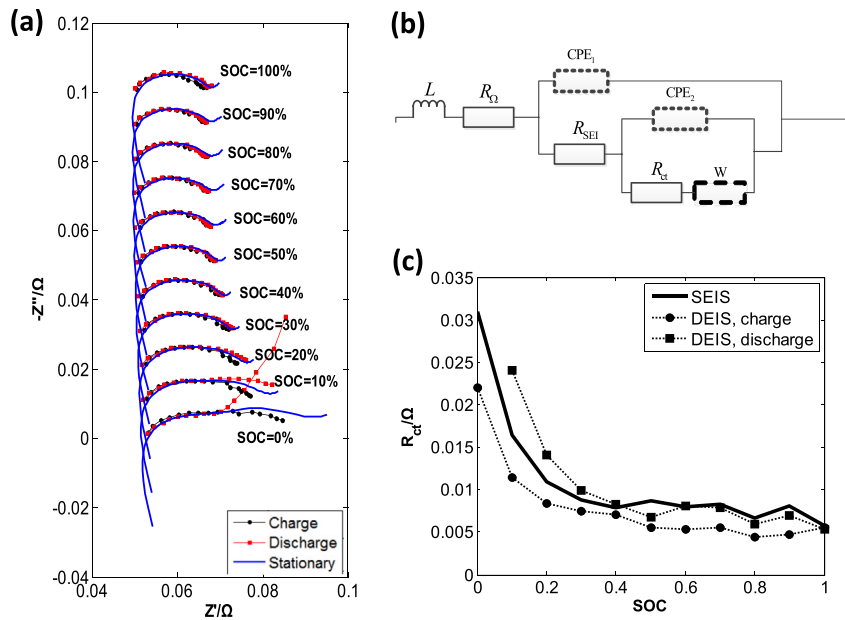


Fig. 3. (a) Impedance spectrum of charging and that of discharging at 11 SOC points from SOC = 1.0 to SOC = 0.0 in a step of SOC = 0.1. It should be noted that in order to discriminate the impedance spectrum at different SOCs, the imaginary part of impedance is artificially shifted by 0.1SOC Ω as a function of SOC. (b) The equivalent electric circuit to simulate the impedance spectrum. L is the inductance, R_Ω , R_{SEI} , R_{ct} correspond to the ohmic resistance, solid electrolyte interphase (SEI) resistance and charge transfer resistance, respectively. CPE denotes the constant phase element. W represents the Warburg element. (c) The charge transfer resistance, R_{ct} , of stationary EIS (SEIS) and DEIS.

During the DEIS measurement, the applied current, $I_{DC} + I_{AC}$, is much larger than the applied current I_{AC} in SEIS measurement. Therefore, the η during DEIS is more significant than that during SEIS. Based on the Eq. (1), the R_{ct} of SEIS exceeds that of DEIS. The exception that when the SOC is smaller than 0.4 during discharging the R_{ct} of DEIS is greater than that of SEIS could be attributed to the depletion of lithium-ions in the anode electrode which magnifies the battery impedance.

(2) The impedance of charging is smaller than that of discharging.

Fig. 3(a) shows that the DEIS of charging shrinks when compared with that of discharging, indicating that the R_{ct} of charging is smaller than that of discharging, which is shown in Fig. 3(c). Although the electrodes are at the same averaged SOC, the surface lithium-ion concentration in the positive electrode during charging is smaller than that during discharging. As i_0 depends on the surface concentration and R_{ct} correlates with i_0 as illustrated in Eq. (1), therefore, this surface concentration deviation causes the differences [13].

(3) A dramatic increase of impedance near SOC = 0. One can notice the “tail-upward” of the impedance near SOC = 0, especially during discharging. As mentioned above, the exchange current density (i_0) depends on the surface concentration of lithium-ions. And i_0 of the positive electrode is decreasing when SOC approaches 0, therefore, the corresponding R_{ct} is increasing. Assuming that the positive electrode dominates the cell impedance, then, one can expect that the impedance increases near SOC = 0.

3.3. Discussion

In this section, the merits and disadvantages of the present DEIS method are analyzed.

The DEIS method in Refs. [6–8] measures the impedance at a set of frequencies point by point successively during charging/discharging, and a single DEIS measurement usually needs several minutes depending on the frequency range and point. As a result,

each DEIS are actually obtained at an SOC range, that is, in the impedance spectrum, the impedance at different frequencies are the results at different SOCs. In order to compare the charge–discharge reactions as the same SOC point, a time axis needs to be introduced, and then the DEIS of each SOC point is interpolated based on the assumption that the battery's state and parameter's spaces are continuous. However, phase change can bring abrupt variations to the battery's parameters. In this regard, the precision of the method in Refs. [6–8] may be influenced at phase transformation points. However, in the present method, the impedance at a certain frequency is continuously monitored during charging/discharging every several seconds. Therefore, using this method, the possible phase change can be captured and considered in comparison between the charge–discharge reactions, with an improved accuracy.

The DEIS method in Ref. [11] measures the impedance spectrum with simultaneous excitation of multiple perturbation frequencies. Although it is also capable of obtaining the DEIS almost at an SOC point, the method in Ref. [11] suffers from the difficulties in designing appropriate amplitudes and phase angles for each perturbation signal. On the contrary, the present method in this study is much easier to implement and can readily be conducted with a commercial instrument such as the Autolab used here.

However, the present DEIS method needs to cycle the cell for several times to measure the impedance of each selected frequency. Therefore, one may concern that the cell degradation during the measurement will affect the accuracy of the impedance spectrum collected from the results of different cycles. However, on one hand, the degradation rate of the commercial cell used in this study during the initial stage is very slow, on the other hand, to decrease the cycle number and so as to suppress the degradation, only 5 points were selected per decade and the frequency range was limited to 1000–1 Hz. While in the SEIS test, 10 points per decade and a frequency range of 10,000–0.01 Hz were designed to get a detailed EIS of the cell. As shown in Fig. 4, the cell capacity almost keep constant and negligible degradation can be found after 16 cycles during the DEIS test. In addition, the EIS test at two SOC ends,

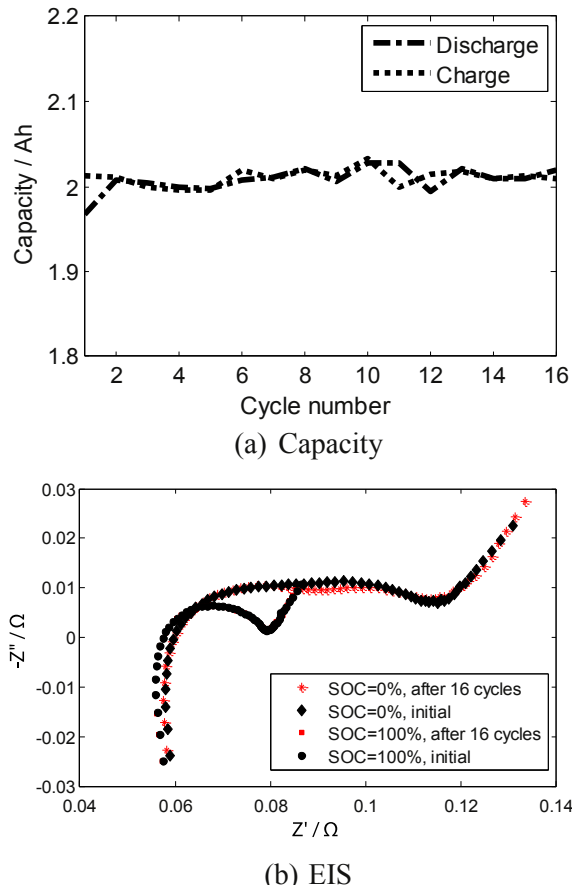


Fig. 4. (a) The evolution of the capacity during the DEIS measurement; (b) the comparison between the EIS of the initial state and that after 16 cycles. Z' and Z'' represent the real and imaginary part of impedance, respectively. The frequency range are 10^5 Hz– 10^{-2} Hz.

in a wide frequency range of 10^5 Hz to 10^{-2} Hz, indicates that the cell impedance also varies to very little extent before and after the DEIS measurement.

Regarding the constant current, a value of 1 A, that is, 0.5 C, was selected in the DEIS measurement. This particular current rate results from a trade-off between the test duration and the stability of the cell state. A larger current will shorten the test duration, while result in a drastic transient change in the cell state. As shown in our previous study [13], a larger current decreases the charge transfer resistance.

Additionally, a stable three-electrode system is preferred to get a separate impedance response of a single electrode, and it is our next step.

4. Conclusion

In this study, we proposed a novel implementation of DEIS method by conducting continuous impedance measurement of a single frequency on a full SOC range during charging or discharging, and by repeating the cycling process for other multiple frequencies. Then, the impedance spectrum of different frequencies at each specific SOC during charging and discharging could be extracted. Using the proposed method, we explored the differences between DEIS and SEIS, and the differences between charging and discharging. It is found that: (1) the charge transfer resistance from the DEIS was generally smaller than that from the SEIS in a wide state-of-charge (SOC) range from 0.4 to 1.0, (2) the charge transfer resistance during charging was smaller than that during discharging, (3) a dramatic increase of impedance, especially during discharging, occurred near SOC = 0.

Acknowledgment

This work is supported by the National Natural Science Foundation of China under the grant number of 51207080, the Independent Research Programs of Tsinghua University under the subject number of 2011Z01004, and the China Postdoctoral Science Foundation under the grant number of 2012M510436. In addition, the useful comments from the reviewers are gratefully appreciated.

References

- [1] F. Croce, F. Nobili, A. Deptula, W. Lada, R. Tossici, A. D'Epifanio, B. Scrosati, R. Marassi, *Electrochim. Commun.* 1 (1999) 605–608.
- [2] S. Klink, E. Madej, E. Ventosa, A. Lindner, W. Schuhmann, F. La Mantia, *Electrochim. Commun.* 22 (2012) 120–123.
- [3] Z. Ogumi, *Electrochemistry* 78 (2010) 319–324.
- [4] J. Zhang, J. Lee, *J. Power Sources* 196 (2011) 6007–6014.
- [5] J. Zhang, J. Huang, Z. Li, B. Wu, Z. Nie, Y. Sun, F. An, N. Wu, *J. Therm. Anal. Calorim.* 117 (2014) 447–461.
- [6] M. Itagaki, N. Kobari, S. Yotsuda, K. Watanabe, S. Kinoshita, M. Ue, *J. Power Sources* 135 (2004) 255–261.
- [7] M. Itagaki, N. Kobari, S. Yotsuda, K. Watanabe, S. Kinoshita, M. Ue, *J. Power Sources* 148 (2005) 78–84.
- [8] Z.B. Stoyanov, B.S. Savova-Stoyanov, *J. Electroanal. Chem. Interfacial Electrochem.* 183 (1985) 133–144.
- [9] P. Chenebault, D. Vallin, J. Thevenin, R. Wiart, *J. Appl. Electrochem.* 19 (1989) 413–420.
- [10] T. Osaka, T. Momma, T. Tajima, *Denki Kagaku* 62 (1994) 350–351.
- [11] J. Ryl, K. Darowicki, P. Slepški, *Corros. Sci.* 53 (2011) 1873–1879.
- [12] M. Darab, P.K. Dahlstrøm, M.S. Thomassen, F. Seland, S. Sunde, *J. Power Sources* 242 (2013) 447–454.
- [13] J. Huang, J. Zhang, Z. Li, S. Song, N. Wu, *Electrochim. Acta* 131 (2014) 228–235.